Available online at www.sciencedirect.com
ScienceDirect
Catalysis Today 133–135 (2008) 493–501
CATALYSIS TODAY
www.elsevier.com/locate/cattod

Combustion of volatile organic compounds over supported manganese oxide: Influence of the support, the precursor and the manganese loading

Fabiola N. Aguero [a], Alberto Scian [b], Bibiana P. Barbero [a], Luis E. Cadús [a,*]

[a] *Instituto de Investigaciones en Tecnología Química (INTEQUI), UNSL, CONICET, Casilla de Correo 290, 5700 San Luis, Argentina*
[b] *Centro de Tecnología de Recursos Minerales y Cerámica (CETMIC), Camino Parque Centenario y 506, 1897 Manuel B. Gonnet, Buenos Aires, Argentina*

Available online 7 January 2008

Abstract

Manganese oxide catalysts supported on Al_2O_3 and $Mg–Al_2O_3$ composite were prepared from two different precursors, manganese acetate and manganese nitrate, with two manganese loadings. Catalytic performance was evaluated in ethanol combustion, which is a volatile organic compound used as solvent in print industries and a potential fuel for vehicles. The most active and selective catalysts to total oxidation were those prepared from manganese acetate. By means of a wide physicochemical characterization by X-ray diffraction (XRD), X-ray fluorescence (XRF), X-ray photoelectron spectroscopy (XPS), temperature-programmed reduction (TPR), Raman spectroscopy, scanning electron microscopy (SEM), and specific surface area measurements, it was found that the best catalytic performance was obtained when manganese oxide species are highly dispersed on the catalyst surface. The formation of these surface species depends mainly on the manganese precursor and also on the support and the manganese loading.

Keywords: Supported manganese oxide catalysts; Characterization; Complete oxidation

1. Introduction

Volatile organic compounds (VOCs) and NO_x are the main contribution to the atmospheric pollution. When great volumes of gases with low concentrations of VOC have to be treated, the catalytic oxidation is preferred. Platinum and palladium are the most commonly used catalysts [1]. However, metal oxides such as manganese oxides have demonstrated a catalytic activity as good as the one of the noble metals. Moreover, they are a cheaper alternative and have a higher sinterised resistance [2].

Considering that the main sources of VOC are vehicles and industries that use solvents, it is important to evaluate the catalytic performance in ethanol combustion, due to two main reasons: (i) this is a potential fuel for vehicles and (ii) with ethyl acetate, they are both widely used solvents.

Industrial application of VOC catalytic combustion process involves great volumes of gases therefore, it is essential to deposit the catalyst on a structured support to avoid high-pressure drops. The most studied supports are monoliths, which are usually made of ceramic or metal materials, covered with a carrier, alumina, that acts as a support of the active phase [3].

It is widely known that deposition of a metallic oxide on an inert support leads to a catalyst with better catalytic performance than the oxide as a bulk catalyst. In part, this is due to the high surface area that supports present. However, the main reason from the catalytic behaviour point of view is the oxide specie type generated on the surface, which depends on the dispersion of the active phase and its interaction with the support.

In the present work, catalysts based on manganese oxides supported on alumina and $Mg–Al_2O_3$ composite are studied. These oxides can be used as carriers for monolithic catalysts. In addition, the influence of the support nature (composition, surface acidity, etc.), the precursor nature (organic, inorganic)

* Corresponding author. Fax: +54 2652 426711.
E-mail address: lcadus@unsl.edu.ar (L.E. Cadús).

0920-5861/$ – see front matter © 2007 Elsevier B.V. All rights reserved.
doi:10.1016/j.cattod.2007.11.044

and the active phase loading is studied. The catalytic performance was evaluated in ethanol total combustion, selected as a VOC probe molecule.

2. Experimental

2.1. Supports preparation

2.1.1. Al_2O_3

An aluminium hydroxide gel was prepared by a chemical reaction between pseudobohemite AlO(OH) and acetic acid in aqueous alcoholic medium. The gel was stabilised for 48 h, diluted one in two parts (w/w) in alcohol and finally dried. The dried sample was calcined at 1000 °C for 10 min.

2.1.2. $Mg–Al_2O_3$ composite

The alumina prepared as described above was dried at 70 °C during 2 h under vacuum and then impregnated to incipient wetness with aqueous solutions of $Mg(NO_3)$ at 50 °C. The concentration of the solution was the necessary to obtain 10 wt% of MgO. The sample was dried at 70 °C overnight and then calcined from room temperature to 450 °C at a heating rate of 3 °C/min being kept at this temperature for 3 h. Due to the partial dissolution of MgO when it is impregnated with an aqueous solution, a hydroxylation was made following the proceeding reported by Llorente et al. [4]. The support was suspended in an aqueous ammonia solution at pH 11.9 and after being stirred for 2 h, the solvent was withdrawn in a rotary vacuum desiccator at 50 °C, and finally calcined at 450 °C for 3 h.

2.2. Catalysts preparation

The catalysts were prepared by impregnation to incipient wetness of the supports (Al_2O_3 and $Mg–Al_2O_3$), previously dried at 137 °C for 3 h, with aqueous solutions of $Mn(NO_3)_2{\cdot}4H_2O$ (Merck) or $Mn(CH_3COO)_2{\cdot}2H_2O$ (Fluka). The impregnation was carried out in multiple stages with drying in between at 100 °C for 1 h. The amount of added solution was the necessary to obtain a manganese loading equivalent to one or three theoretical monolayers of MnO_x. Finally, the samples were dried at 70 °C overnight and calcined at 500 °C for 3 h. The obtained catalysts were called xMn/Al_2O_3(p) and xMn/Mg–Al_2O_3(p), where $x = 1$ or 3 represents the manganese amount (equivalent amount to one or three monolayers of MnO_x) and p = ''n'' or ''a'' for manganese nitrate or manganese acetate, respectively.

2.3. Catalysts characterization

2.3.1. Isoelectric point (IEP)

The IEP measurements were carried out in a Zeta Meter System 3.0 apparatus, using 30 mg of sample dispersed in a 10^{-3} M KCl solution. The pH was adjusted with either 10^{-2} M KOH or HCl solutions.

2.3.2. Ammonia temperature-programmed desorption (NH_3-TPD)

A quartz tubular reactor and a thermal conductivity detector (TCD) as detector were used. The adsorption step was carried out in a pure ammonia flow at room temperature for 1 h. Then, the sample was swept in pure helium for 30 min. The desorption was performed in a pure helium flow of 30 ml min^{-1}, from 30 °C to 700 °C at a heating rate of 10 °C min^{-1}.

2.3.3. X-ray fluorescence (XRF)

A PW 1400 Philips instrument was used. The calibration was made with mixtures of oxides with known concentrations.

2.3.4. BET-specific surface area measurements (S_{BET})

The specific surface area of the catalysts was calculated by the BET method from the nitrogen adsorption isotherms obtained at 77 K. A Micromeritics Accusorb 2100E apparatus was used.

2.3.5. X-ray diffraction (XRD)

XRD patterns were obtained by using a Rigaku diffractometer operated at 30 kV and 25 mA by employing Cu Kα radiation with nickel filter ($\lambda = 0.15418$ nm).

2.3.6. Laser Raman spectroscopy (LRS)

A JASCO TRS600SZP multichannel spectrometer with an argon ion (514.5 nm) operated at 80 mW was used.

2.3.7. Temperature-programmed reduction (TPR)

The TPR was performed in a quartz tubular reactor using a TCD as detector. A 100 mg sample was used. The reducing gas was a mixture of 5 vol.% H_2/N_2, at a total flow rate of 30 ml min^{-1}. The temperature was increased at a rate of 5 °C min^{-1} from room temperature to 700 °C.

2.3.8. X-ray photoelectron spectroscopy (XPS)

A VG Scientific Escalab 200A equipment with an Al anode, $E_0 = 15$ keV (300 W) was employed. The C 1s peak at 285 eV was taken as reference.

2.3.9. Scanning electron microscopy (SEM)

A JEOL JSM 6301F microscope was employed. The powder samples were pelletized and coated with a thin conductive carbon layer. The analyses were made by means of back-scattered electrons.

2.4. Catalytic evaluation

A quartz reactor of fixed bed at atmospheric pressure was used. The reaction temperature, measured with a thermocouple in the centre of the catalytic bed, was varied from 90 °C until total conversion of ethanol was obtained. Data were obtained in steady state. A sample of 300 mg (0.5–0.8 mm particle diameter) diluted with glass particles of the same size in a ratio 1:5 was used. The feed was a mixture of molar ratio $C_2H_5OH:O_2:He = 1:20.8:78.2$ at a total flow rate of 100 ml min^{-1}. The reagents and reaction products were

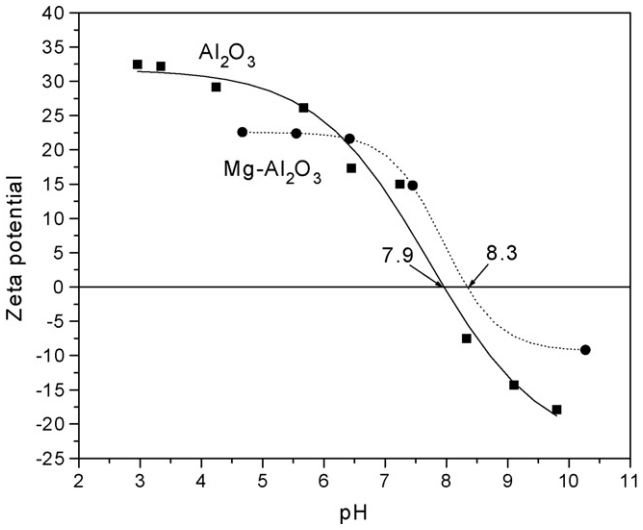

Fig. 1. Zeta potential vs. pH curves for the supports.

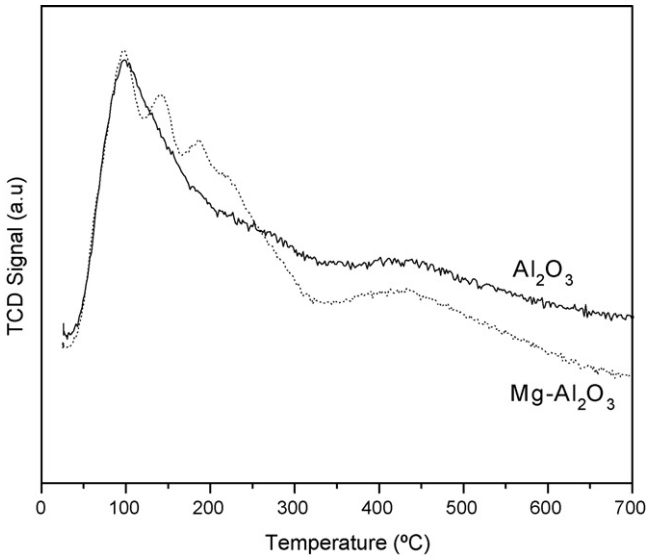

Fig. 2. Temperature-programmed desorption of ammonia for the supports.

analyzed online by a Shimadzu GC9A gas chromatograph equipped with a Porapak T column and a thermal conductivity detector.

The conversion of ethanol, $X(\%)$, was defined as

$$X\,(\%) = \frac{\mathrm{EtOH_{in}} - \mathrm{EtOH_{out}}}{\mathrm{EtOH_{in}}} \times 100$$

3. Results

3.1. Isoelectric point

Zeta potential versus pH curves are presented in Fig. 1. The isoelectric points for the Al_2O_3 and Mg–Al_2O_3 composite are 7.94 and 8.30, respectively.

3.2. Temperature-programmed desorption of ammonia (NH_3-TPD)

The results are shown in Fig. 2. The Al_2O_3 TPD profile is characterized by one strong NH_3 desorption peak at about 100 °C and weaker peaks at around 250 °C and 425 °C. These peaks were assigned to the desorption of coordinately held NH_3 from Lewis acid sites of different strengths [5]. The Mg–Al_2O_3 TPD curve presents some differences regarding to that of Al_2O_3 in the region of the weaker acid sites. It exhibits a splitted broad peak with maxima at 100 °C, 140 °C, 180 °C and 220 °C. A weaker peak at 425 °C as for Al_2O_3 is also observed.

3.3. X-ray fluorescence

Theoretical and experimental manganese content values are shown in Table 1. In the case of the catalysts with a manganese loading equivalent to one theoretical monolayer, the values determined experimentally (approximately 11 wt% Mn) are in reasonable agreement with the theoretical values. For the catalysts with higher manganese loading, the manganese content (about 20 wt% Mn) is quite lower than the expected one, regardless on the precursor and the support.

3.4. Specific surface areas (S_{BET})

Specific surface areas are presented in Table 1. Al_2O_3 and Mg–Al_2O_3 composite supports have the same surface area. Supported manganese catalysts prepared from manganese

Table 1
Elemental composition from XRF, specific surface areas (S_{BET}), hydrogen consumption from TPR and catalytic activity

Catalyst	Mn content (wt% Mn)		S_{BET} (m^2/g)	Hydrogen consumption		Catalytic activity	
	Theoretical	Experimental		μmol H_2	μmol H_2/mg Mn	T_{50}	T_{80}
Al_2O_3	–	–	102.5	–	–	–	–
Mg–Al_2O_3	–	–	102.5	–	–	–	–
1Mn/Al_2O_3(n)	12.45	11.3	87.9	133.8	11.2	235	250
3Mn/Al_2O_3(n)	37.3	22.7	64.0	206.0	8.3	217	235
1Mn/Mg–Al_2O_3(n)	12.45	11.2	85.2	121.7	10.7	220	242
3Mn/Mg–Al_2O_3(n)	37.3	18.5	59.3	208.8	10.5	217	235
1Mn/Al_2O_3(a)	12.45	10.0	101.4	88.8	8.7	192	215
3Mn/Al_2O_3(a)	37.3	19.2	98.6	135.0	6.9	177	200
1Mn/Mg–Al_2O_3(a)	12.45	11.8	97.9	92.5	7.8	184	212
3Mn/Mg–Al_2O_3(a)	37.3	19.9	97.9	130.4	6.4	192	220

T_{50} and T_{80}: reaction temperatures corresponding to 50% and 80% of ethanol conversion, respectively.

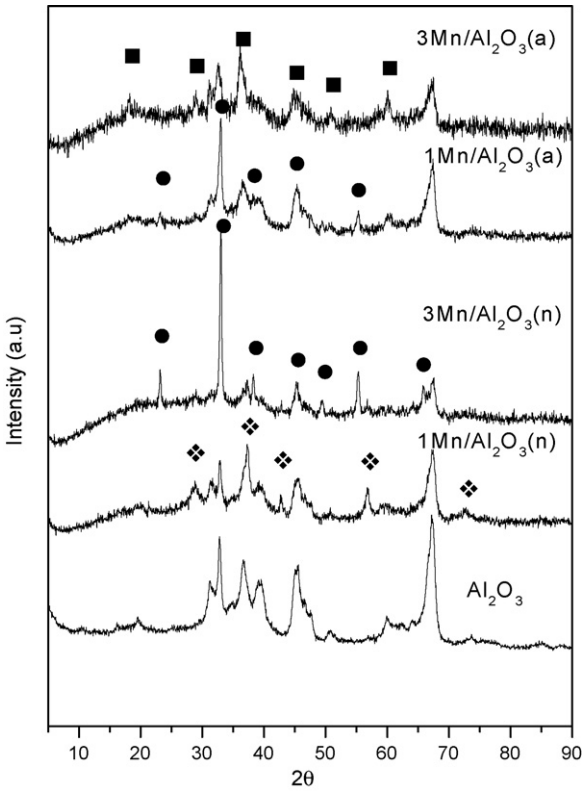

Fig. 3. X-ray diffractograms for the Al_2O_3 support and the xMn/Al_2O_3(p) catalysts. (❖) MnO_2 PDF file 24-735; (●) Mn_2O_3 PDF file 24-508; (■) Mn_2O_3 PDF file 18-803.

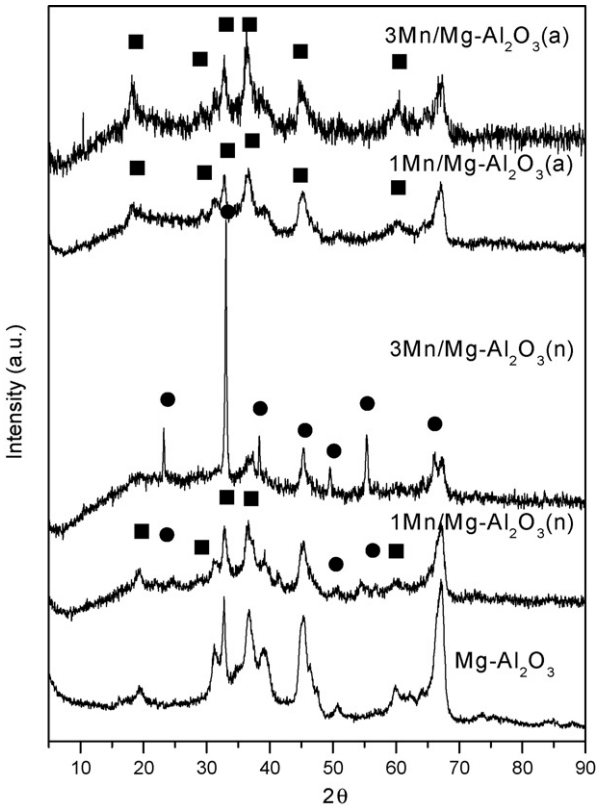

Fig. 4. X-ray diffractograms for the Mg–Al_2O_3 support and the xMn/Mg–Al_2O_3(p) catalysts. Symbols as in Fig. 3.

nitrate show a decrease of the specific surface area when manganese loading increases. The specific surface area of the catalysts prepared from acetate very slightly decreases when manganese loading increases.

3.5. X-ray diffraction

Figs. 3 and 4 show the X-ray diffractograms for the xMn/Al_2O_3(p) and xMn/Mg–Al_2O_3(p) catalysts and their respective supports. The diffraction lines of the Al_2O_3 support were identified as transition phases θ-Al_2O_3 (PDF file 35-121) and δ-Al_2O_3 (PDF file 4-877). Mg–Al_2O_3 support presents similar X-ray diffractogram to that of the Al_2O_3. Other diffraction lines were not observed. The diffractograms of the supported manganese catalysts exhibit several differences depending on the precursor, on the manganese loading, and also on the support. The diffractograms of the catalysts with lower manganese loading conserve the diffraction lines of the support and exhibit additional lines corresponding to manganese oxides. For 1Mn/Al_2O_3(n), these lines were identified as MnO_2 phase (PDF file 24-735) while with manganese acetate as precursor, they were assigned to Mn_2O_3 (PDF file 24-508). On the Mg–Al_2O_3 support, the additional lines were identified as Mn_2O_3 (PDF files 24-508 and 18-803). At higher manganese loadings, support influence was not observed, but the crystallinity was very different depending on the precursor. With nitrate as precursor, the formation of crystalline Mn_2O_3 (PDF file 24-508) and the most intense diffraction line of the support were observed. With acetate, the crystallinity is very low and the resulting manganese oxide could be Mn_2O_3 (PDF file 18-803).

3.6. Laser Raman spectroscopy (LRS)

The spectra are shown in Figs. 5 and 6. All present a broad band centred at 588 cm^{-1}. On this band, other bands and shoulders, which intensities and positions mainly depend on the precursor, are observed. The spectra of the catalysts prepared from the nitrate precursor exhibit a weak band at 665 cm^{-1} which intensity decreases slightly with the increase of the manganese loading. The support influence is not appreciable. Catalysts prepared on Al_2O_3 and impregnated with acetate present a Raman band at 644 cm^{-1} which intensity notably increases with the manganese loading. On the contrary, in the spectra of the catalysts prepared on Mg–Al_2O_3 support the band is centred at 652 cm^{-1} and the intensity slightly increases with the manganese loading. The assignation of these bands is not a straightforward task since diverse manganese oxide phases present signals in the 640–660 cm^{-1} region [6,7]. Kapteijn et al. [7] reported Raman spectra of Al_2O_3-supported manganese oxide with a main band centred at 650–653 cm^{-1} when manganese nitrate was used as precursor, and a broader band centred at 637 cm^{-1} for the catalysts prepared from manganese acetate. On the basis of an average stoichiometry from XPS, they assigned these bands to the highly dispersed Mn_2O_3 phase. In a study about manganese oxide supported on

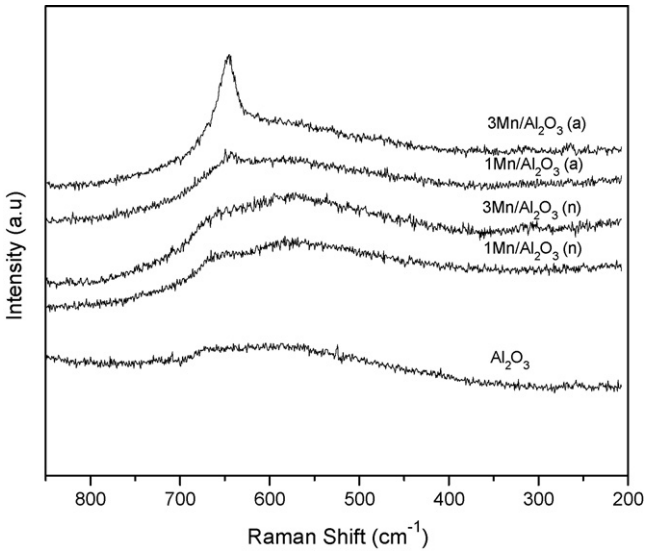

Fig. 5. Raman spectra for the xMn/Al_2O_3(p) catalysts.

several supports (Al_2O_3, ZrO_2, TiO_2 and SiO_2), Radhakrishman et al. [8] detected Raman bands at 661 cm^{-1} for MnO_x/Al_2O_3 and to 664 cm^{-1} for MnO_x/SiO_2. They assigned them to dispersed manganese oxide species but they could not assure the oxidation state of the manganese oxide. These different results demonstrate that the Raman bands position and intensity of the supported manganese oxides depend on the precursor and the manganese loading as well as on the support nature.

3.7. Temperature-programmed reduction

The TPR profiles are presented in Fig. 7. The catalysts prepared from nitrate exhibit two reduction signals. The first one (at 340–360 °C) slightly shifts to lower temperatures with the increase of manganese loading. The second signal is a single peak which appears at 430 °C for low manganese loading and at 465–470 °C when the manganese loading increases. The intensity of the second signal increases with the manganese content. The catalysts prepared from acetate present a main reduction signal at 420 °C which intensity increases with the manganese loading. Furthermore, other less intense signals at low reduction temperature are observed.

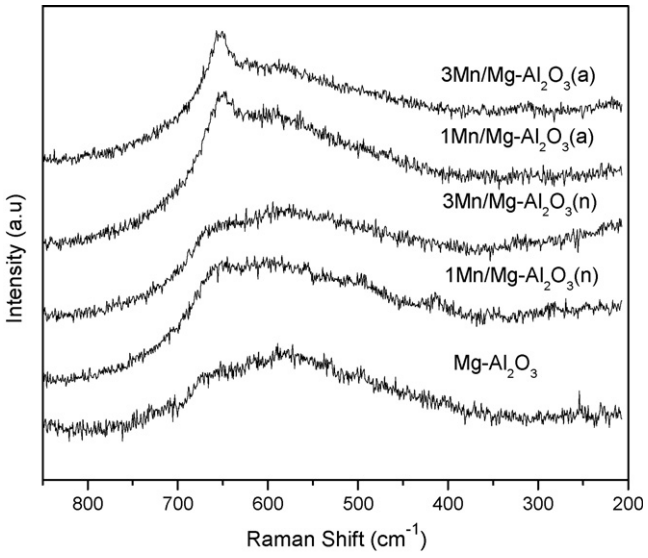

Fig. 6. Raman spectra for the xMn/Mg–Al_2O_3(p) catalysts.

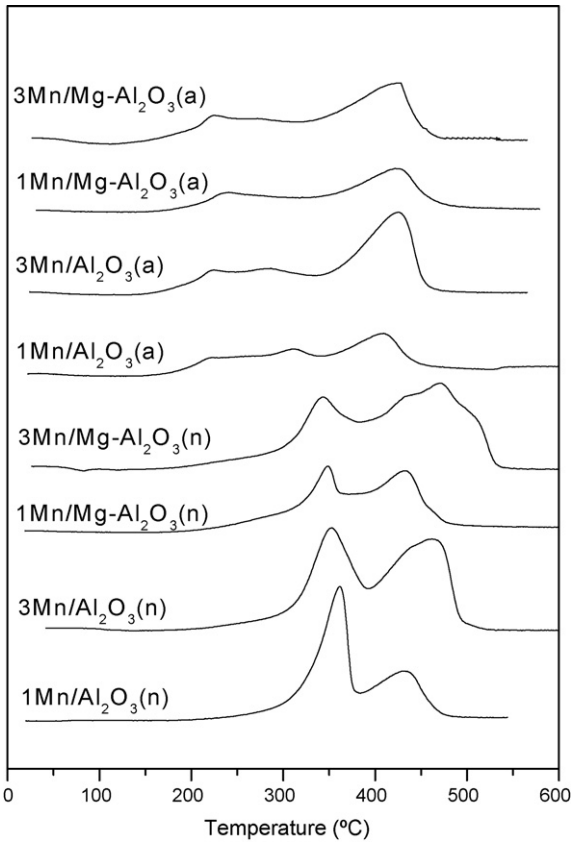

Fig. 7. Temperature-programmed reduction profiles.

The hydrogen consumption is shown in Table 1. As expected, it increases with the increase of manganese loading. The catalysts prepared from nitrate consume more hydrogen than those prepared from acetate. When the hydrogen consumption per manganese mass unit (μmol H_2/mg Mn) is considered, the catalysts prepared from nitrate consume, in average, approximately 10.2 μmol H_2/mg Mn while those prepared from acetate consume 7.5 μmol H_2/mg Mn.

3.8. X-ray photoelectron spectroscopy

The results are presented in Table 2. The Mn/Al and Mn/(Al + Mg) atomic ratios strongly vary depending on the precursor. With nitrate as precursor, these atomic ratios decrease with the increase of the manganese loading. In contrast, with acetate as precursor, they increase with the manganese loading. The values for the catalysts on Mg–Al_2O_3 are higher than those on Al_2O_3 considering equal manganese loading and precursor. The Mg/Al atomic ratio for the Mg–Al_2O_3 support is about 0.3 and this ratio increases to approximately 0.4 for the catalysts prepared from nitrate and to 1.15 for those prepared from acetate. The catalysts prepared

Table 2
Atomic ratios and binding energies (E_b) from XPS

Catalyst	Mn/Al	Mn/(Al + Mg)	Mg/Al	E_b Mn $2p_{3/2}$ (eV)
Al_2O_3	–	–		–
Mg–Al_2O_3	–	–	0.287	–
1Mn/Al_2O_3(n)	0.027	–		652
3Mn/Al_2O_3(n)	0.017	–		650
1Mn/Mg–Al_2O_3(n)	0.052	0.034	0.524	652
3Mn/Mg–Al_2O_3(n)	0.042	0.031	0.350	648
1Mn/Al_2O_3(a)	0.095	–		643–647
3Mn/Al_2O_3(a)	0.209	–		648
1Mn/Mg–Al_2O_3(a)	0.145	0.075	0.917	647
3Mn/Mg–Al_2O_3(a)	0.253	0.106	1.390	645.5

from nitrate present a higher binding energy of Mn $2p_{3/2}$ peak than those prepared from acetate.

3.9. Scanning electronic microscopy

The SEM micrographs acquired by means of backscattered electrons mode are shown in Fig. 8. The obtained imaging is dependent on atomic number contrasts among the different constituents of the sample. The bright zones represent heavy elements while the dark zones correspond to light elements. Thus, the bright zones can be assumed as manganese oxide species and the dark ones as the support.

3.10. Catalytic activity

The results of catalytic activity in ethanol combustion are presented in Figs. 9 and 10 and Table 1. As it is observed in Fig. 9, the catalysts prepared from manganese acetate are markedly more active than those prepared from manganese nitrate in the whole range of reaction temperatures. The oxidation reaction starts at 130–150 °C on the catalysts prepared from nitrate and at temperatures below 100 °C on those prepared from acetate. Comparing T_{50} and T_{80}, reaction temperatures corresponding to 50% and 80% conversion, respectively, a difference of 25–40 °C is observed for both supports and the same manganese loading.

Regarding to the manganese loading, the higher activity of the catalysts supported on Al_2O_3 was obtained with the higher manganese loading. By contrast, the catalysts supported on Mg–Al_2O_3 did not show much influence of the manganese loading and even, the 3Mn/Mg–Al_2O_3(a) catalyst was slightly less active than the 1Mn/Mg–Al_2O_3(a) catalyst. Regarding to

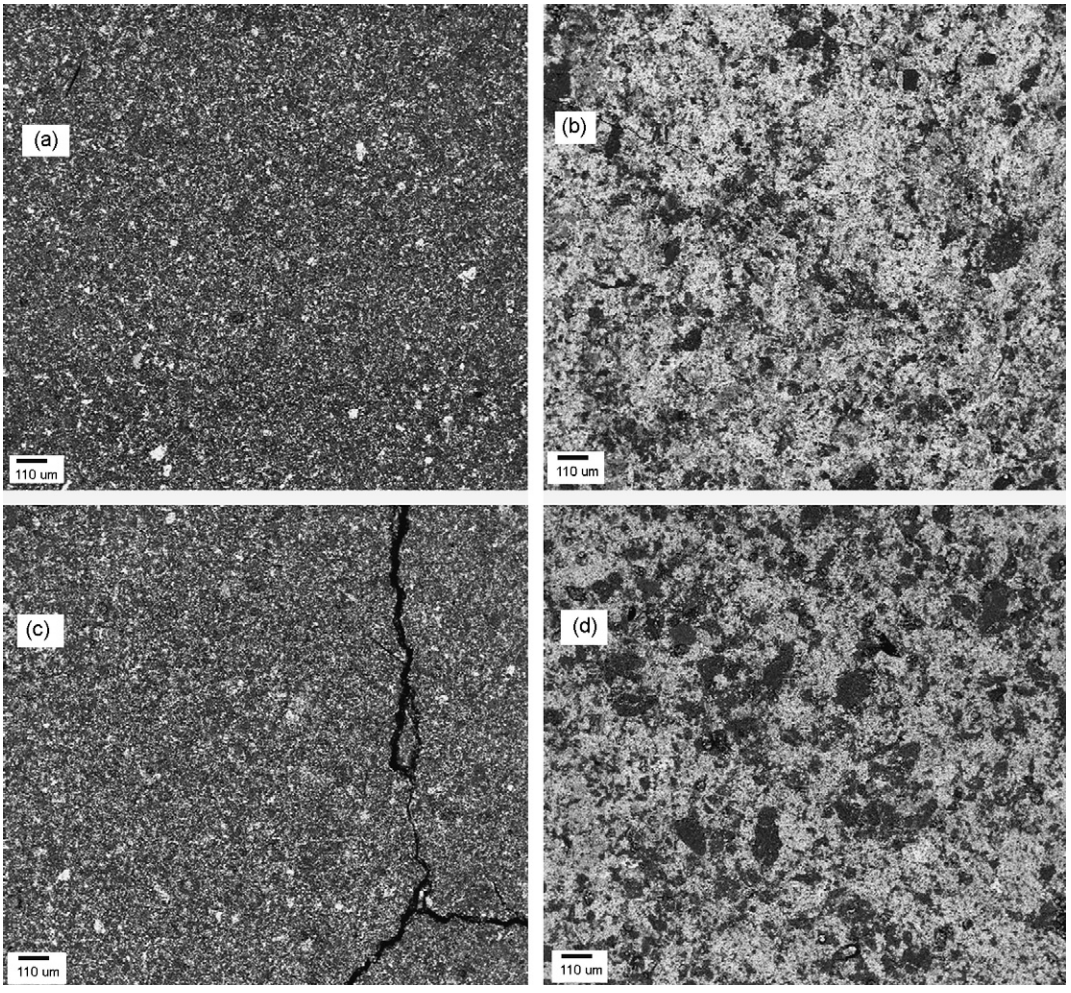

Fig. 8. SEM micrographs for (a) 3Mn/Al_2O_3(n); (b) 3Mn/Al_2O_3(a); (c) 3Mn/Mg–Al_2O_3(n); and (d) 3Mn/Mg–Al_2O_3(a) catalysts.

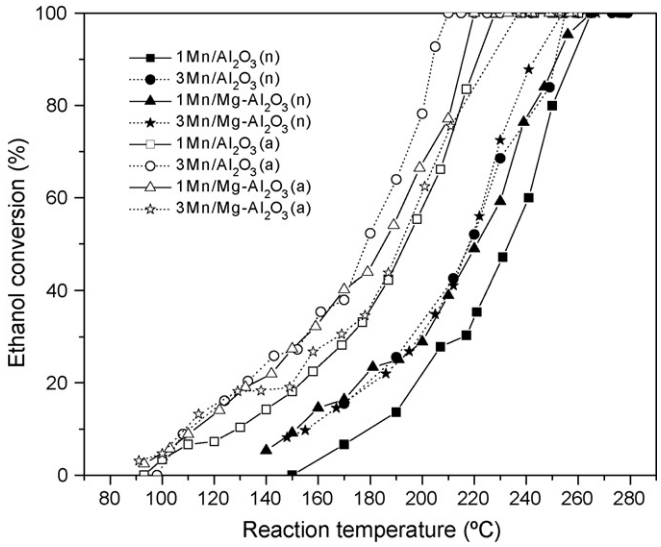

Fig. 9. Ethanol conversion as a function of reaction temperature.

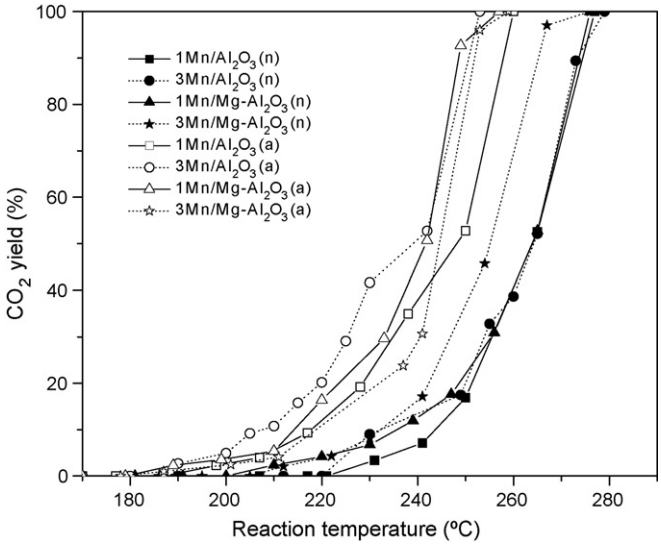

Fig. 10. Yield to CO_2 as a function of reaction temperature.

the support effect, it was observed that the catalysts with low manganese loading were more active when the support was Mg–Al_2O_3 composite. At higher manganese loadings, there was not effect of the support when impregnating with nitrate, but in the case of acetate, the highest activity is obtained on Al_2O_3. In fact, the most active catalyst is 3Mn/Al_2O_3(a).

4. Discussion

The transition alumina θ–δ-Al_2O_3 used as support in this work was prepared following a very interesting method since a relatively high-specific surface area was obtained despite the high calcination temperature (1000 °C). The modification of the alumina with a second oxidic phase has been evaluated in several cases giving very promising results [9,10]. In this work, an Mg–Al_2O_3 composite was prepared from the same alumina used as support. The composite resulted texturally and structurally similar to the original alumina. This fact greatly facilitates the subsequent comparison between the supports.

Generally, the mixed oxides present different surface characteristics from those of the pure oxides. In fact, a modification of the isoelectric point and some differences in the weaker acid sites were observed. The change of the acid–base properties can allow to a modification of the anchoring centres for the surface oxide species constituting the active phase of the catalyst. Thus, a higher dispersion and stability of the supported oxide layer could be achieved and the catalytic behaviour could be affected.

The dispersion of the surface oxide species and its interaction with the support are also determined by the precursor salt employed during the impregnation, the nature of the solvent, the solution pH, among other variables. Furthermore, the loading of active phase deposited on the support can affect the catalytic activity. A low loading (lower than the theoretical monolayer) can generate very active, non-crystalline surface oxide species. However, a low-concentration of these species will give very low overall activity. On the contrary, very high loading leads to the formation of a crystalline oxide layer similar to the bulk oxide, disappearing in this way, the effects of a supported oxide. Then, the choice of an optimal loading of active phase requires a compromise solution. In this work, we study the influence of the precursor and the manganese loading on the nature and the dispersion of the oxide phase supported on Al_2O_3 and the Mg–Al_2O_3 composite as well as the effect of these variables on the catalytic performance.

The catalysts prepared in this work showed an excellent behaviour in ethanol combustion (Figs. 9 and 10 and Table 1). The highest catalytic activity of the catalysts prepared from manganese acetate is manifested by a 25–40 °C difference in the reaction temperature lower than the corresponding one to the catalyst prepared from manganese nitrate. This temperature difference becomes important when great gaseous effluent volumes to be preheated in an actual process are considered.

The ethanol combustion occurs through an intermediate, acetaldehyde, which is a volatile organic compound more noxious for human health than ethanol. Then, a relevant aspect is the selectivity to total oxidation (yield to CO_2). As shown in Fig. 10, the catalysts prepared from manganese acetate are more selective to CO_2 than those prepared from nitrate. Clearly, the acetate precursor generates more active and selective manganese oxide species than that obtained from manganese nitrate.

The differences observed when the active phase loading and the support are varied indicate that these factors influence on the definition of the catalyst surface and consequently, on the catalytic performance. This influence is less important than that of the manganese precursor.

With the aim to explain the catalytic activity results and to determinate the most convenient surface architecture of the manganese oxide for the ethanol combustion, an exhaustive physicochemical characterization of the catalysts was carried out.

Firstly, the nature of the supported manganese oxide attempted to be identified by means of XRD. In the diffractograms of the catalysts with low manganese content,

the diffraction lines of low intensity corresponding to the manganese oxides indicate that the supported oxide layer is amorphous or the crystallites are very small. At high manganese loading, the diffractograms present differences depending on the precursor. Evidently, the manganese precursor has an important influence on the definition of the supported manganese oxide layer. The nitrate precursor favours the formation of a crystalline manganese oxide, probably as microcrystals, which can be detected by XRD. The poor definition of the diffractograms of the catalysts prepared from acetate indicates that the manganese oxide would be found as dispersed surface manganese oxide species.

This is corroborated by the results from Raman spectroscopy, which is a particularly useful technique to study supported oxide species. Even if the Raman band assignation to a determined manganese oxide presents great difficulty, the detected bands in the spectra of our catalysts prepared from acetate can be assigned to manganese oxide species dispersed on the surface.

Another useful technique to obtain information about the dispersion of the supported active phases and their interaction with the support is the temperature-programmed reduction. In fact, the low-temperature reduction signals in the TPR profiles of the catalysts prepared from acetate would correspond to the reduction of the dispersed manganese oxide species. This observation is in line with the results of XRD and Raman spectroscopy. In the TPR profiles of the catalysts prepared from nitrate, the second reduction signal increases and broadens with the increase of the manganese loading. This would be due to a higher concentration of Mn_2O_3 crystallites and/or to a size growth of these crystallites as it has been deduced from the XRD results. Considering the similarity of the hydrogen consumption per manganese mass unit values, it can be proposed that similar manganese oxide species exist in the catalysts prepared from nitrate regardless on the manganese loading and the support.

The TPR study can also be useful to obtain hints about the oxidation state of the supported manganese oxide. It is expected that the manganese oxides in different oxidation states show differences in the reduction curves and/or the hydrogen consumption. Actually, the catalysts prepared from acetate consume less hydrogen than those prepared from nitrate. This indicates that the MnO_x species obtained from the acetate precursor have a lower average oxidation state than that of the microcrystalline Mn_2O_3 phase resulting of the nitrate precursor. The XPS results are in agreement with this observation. The lower binding energy of Mn 2p in the catalysts prepared from acetate indicates a lower oxidation state [7]. The low hydrogen consumption during the reduction could be considered as a low oxygen amount available in the surface MnO_x species which indicates the existence of oxygen vacancies. The oxygen vacancies are recognised as adsorption–desorption centres for oxygen from the gaseous phase and consequently, they would act as active centres in oxidation reactions.

As the catalysis is a surface phenomenon, the surface properties of the catalysts can be more important than the bulk composition and characteristics. Therefore, surface characteristics of the catalysts such as specific surface area and the dispersion of the active phase on the surface were determined.

The specific surface areas strongly depend on the manganese precursor. For the catalysts prepared from nitrate, the specific surface area decreased with the increase of the manganese loading almost in the same proportion on both supports. By contrast, the catalysts prepared from acetate practically maintained the specific surface areas of the supports. Probably, the impregnation with manganese nitrate provokes a blocking effect of the support pores causing a reduction of the specific surface area. This blocking effect can be produced by accumulation of manganese oxide in the pore mouth or perhaps, the conditions for the impregnation with nitrate (concentration of the precursor salt in the solution, solution pH, drying temperature, etc.) could provoke a sealing of the support pores because of the alumina dissolution [11]. When manganese acetate was used as precursor, drastic decreasing of the specific surface area was not observed. Probably, the higher solution pH (6.7–7.5 [7]) or the nature of the precursor salt hindered the pore sealing conserving the surface area. The low-specific surface area of the catalysts prepared from nitrate can partially explain the low activity of the catalysts. However, this consideration is not enough to explain the results with different manganese loadings. A more suitable way to compare the catalytic performance is considering the dispersion of the manganese oxide layer and its interaction with the support.

The surface atomic ratios Mn/Al and Mn/(Al + Mg) determined by XPS give an idea of the dispersion of the manganese oxide layer. The higher values observed for the catalysts prepared from acetate indicate that the acetate precursor produces a higher dispersion of the MnO_x species. The SEM micrographs corroborate this observation.

In order to evaluate the effect of the support and the manganese loading on the dispersion of the supported oxide layer, the results obtained with each precursor will be analyzed separately since they do not follow the same tendency. With the nitrate precursor, the atomic ratios Mn/Al and Mn/(Al + Mg) decrease with the increase of the manganese loading. This would be due to a lower manganese amount on the surface or a lower manganese dispersion. If the decrease of the specific surface area with the increase of manganese loading occurs because of the pore sealing as discussed above, part of the manganese can be retained within the pore and cannot be accessible to the measurement by XPS. Another possible explanation is that the consecutive depositions of manganese can allow to the growth of the surface manganese oxide aggregates without increasing the surface coverage. In this case, the aggregates can grow until forming manganese oxide crystals. In fact, only the catalysts with higher manganese loading prepared from nitrate show crystalline XRD patterns. With the acetate precursor, the atomic ratios Mn/Al and Mn/(Al + Mg) increase with the manganese loading in a proportion that depends on the support nature. On Al_2O_3, the ratio Mn/Al practically doubles its value as occurs with the manganese content determined by XRF. This indicates that the manganese oxide is more

dispersed on the surface than when manganese nitrate is used as precursor. On the contrary, on $Mg–Al_2O_3$, the atomic ratio Mn/(Al + Mg) increases in lower proportion than the manganese content determined by XRF. This shows that when the manganese loading on $Mg–Al_2O_3$ increases, the manganese aggregates tend to grow instead of increasing the surface coverage as occur on Al_2O_3. Considering the notable increasing of the atomic ratio Mg/Al when manganese acetate is used as precursor, it can be deduced that manganese covers preferentially the Al atoms. This indicates that the anchoring sites of manganese to the surface are associated to the support aluminium atoms. Otherwise, when manganese nitrate is used as precursor, the support effect is less significant. The differences in the isoelectric point and/or the surface acid–base properties of the supports would be the cause of the supported manganese oxide dispersion.

On the bases of the characterization results, it can be deduced that the catalytic performance is associated to the nature of the surface manganese oxide species. As it was proposed in [12], the dispersed manganese oxide species able to hold defects such as oxygen vacancies are the responsible of the good catalytic performance.

5. Conclusions

The nature and characteristics of the supported manganese oxide phase strongly depend on the manganese precursor used, and to a lesser extent, on the support and the manganese loading.

With manganese acetate as precursor, highly dispersed manganese oxide species are obtained on the surface. These species are easily reducible and could present oxygen vacancies. With manganese nitrate as precursor, the formation of microcrystalline Mn_2O_3 is favoured.

The catalytic performance in the ethanol combustion on the catalysts prepared from manganese acetate is notably higher than that on the catalysts prepared from manganese nitrate. This can be attributed to the highly dispersed manganese oxide species generated on the surface when the manganese acetate precursor is used.

Acknowledgements

The authors thank the financial support to UNSL, CONICET and ANPCyT of Argentina. The Raman spectra were obtained at the CENACA (Santa Fe, Argentina). XPS and SEM measurements were made thanks to a cooperation programme SECyT (Argentina)–GRICES (Portugal).

References

[1] E. Noordally, J.R. Richmond, S.F. Tahir, Catal. Today 17 (1993) 359.
[2] J. Trawczynski, B. Bielak, W. Mista, Appl. Catal. B 277 (2005) 55.
[3] P. Avila, M. Montes, E. Miró, Chem. Eng. J. 109 (2005) 11.
[4] J.M. Llorente, V. Rives, P. Malet, F.J. Gil-Llambías, J. Catal. 135 (1992) 1.
[5] S. Rajagopal, T.L. Grimm, D.J. Collins, R. Miranda, J. Catal. 137 (1992) 453.
[6] F. Buciuman, F. Patcas, R. Cracium, R.T.D. Zhan, Phys. Chem. Chem. Phys. 1 (1999) 185.
[7] F. Kapteijn, D. van Langeveld, J.A. Moulijn, A. Andreini, M.A. Vuurman, A.M. Turek, J.-M. Jehng, I.E. Wachs, J. Catal. 150 (1994) 94.
[8] R. Radhakrishnan, T. Oyama, J. Chen, K. Asakura, J. Phys. Chem. B 105 (2001) 4245.
[9] R. Zhang, J.A. Schwarz, A. Datye, J.P. Baltrus, J. Catal. 135 (1992) 200.
[10] M.C. Abello, M.F. Gómez, L.E. Cadús, Ind. Chem. Res. 35 (1996) 2137.
[11] G. Patermarakis, N. Papandreadis, Electrochim. Acta 36 (1993) 1413.
[12] M. Baldi, V. Sanchez Escribano, J.M. Gallardo Amores, F. Milella, G. Busca, Appl. Catal. B 17 (1998) 175.